

Temperature dependence of the magnetocrystalline anisotropy energy and projected microscopic magnetic moments in epitaxial CrO₂ films

S. Gold,¹ E. Goering,^{1,*} C. König,² U. Rüdiger,³ G. Güntherodt,² and G. Schütz¹

¹Max-Planck-Institut für Metallforschung, Heisenbergstrasse 3, 70569 Stuttgart, Germany

²II. Physikalisches Institut RWTH Aachen, Huyskenweg, 52074 Aachen, Germany

³Fachbereich Physik, Universität Konstanz, Universitätsstrasse 10, 78457 Konstanz, Germany

(Received 13 January 2005; published 10 June 2005)

Soft x-ray magnetic circular dichroism spectra and *in situ* element specific hysteresis loops of epitaxially grown CrO₂ thin films have been investigated in the temperature range from 25 to 330 K for two different crystallographic projections. The quantitative temperature dependence of the microscopic magnetic moments (spin, orbital, and magnetic dipole term) and the magnetocrystalline anisotropy energy give strong evidence for the validity of the models by Bruno and by van der Laan, which describe the generation of the orbital moment and its relation to the magnetic anisotropy energy.

DOI: 10.1103/PhysRevB.71.220404

PACS number(s): 75.30.Gw, 75.70.-i, 78.70.Dm

Halfmetallic ferromagnets with a high spin polarization at the Fermi energy have been widely investigated in the last years due to their applicability for future spintronic devices.^{1,2} The theoretically predicted 100% (Refs. 3–6) spin polarization for CrO₂ has been verified by superconducting tunneling spectroscopy at $T=1.85$ K (Refs. 7 and 8) and spin-polarized photoemission spectroscopy at $T=293$ K.⁹ Even a very high spin-polarized current has been achieved across a CrO₂/I/Al junction at 400 mK.¹⁰ The oxygen-mediated exchange coupling and the halfmetallic nature are a challenging problem for theoretical descriptions, because of the presence of Cr(3*d*)-O(2*p*) hybridization, double exchange, self-doping, and correlation effects.⁴ CrO₂ is metastable at room temperature, which is a severe problem for surface sensitive spectroscopic investigations.¹¹ Nevertheless, high quality, epitaxially grown thin-film samples of CrO₂ can be prepared¹² that exhibit anisotropic electronic transport properties and a magnetic easy axis along the CrO₂ [001]-direction.¹³ Recently performed oxygen *K* edge x-ray absorption spectroscopy (XAS) on an epitaxially grown CrO₂ (100) film with nearly no Cr₂O₃ contributions gave detailed information about the orbital character of the O 2*p*-like states near the Fermi level and their anisotropic behavior.¹⁴ In addition, high-quality angular-dependent x-ray magnetic circular dichroism (XMCD) results at the Cr $L_{2,3}$ edges have identified different parts of the unoccupied band structure projected along different crystallographic directions.¹⁵ As a key result the influence of the orbital moments and the magnetic dipole term T_Z on the magnetocrystalline anisotropy energy (MAE) has been quantitatively verified. Recently these results have been qualitatively approved for T_Z moment in a theoretical work by Komelj *et al.*¹⁶

The MAE is responsible for very important material properties, such as the direction of the easy axis and the coercive field. One important issue to magnetic storage applications is the superparamagnetic limit, which must be shifted to higher temperatures for future ultrahigh-density data storage applications. For this issue, the MAE is a key property to control this limit.¹⁷ For the orbital moment of 3*d* ferromagnets with

a filled majority band, Bruno had proposed a perturbation theory description, where the small nonquenched total orbital moment is a result of the spin-orbit coupling and the present spin moment.¹⁸ Bruno has further predicted that this interaction of the residual orbital moment with the lattice and the spin moment is the origin of the MAE. This early model has been extended by van der Laan for systems with not completely filled majority 3*d*-band and added the influence of a quadrupolar spin density, the magnetic dipole term T_Z , to the MAE.¹⁹ Those models can be verified or falsified by microscopic measurements of orbital, spin, and dipole term projections in element specific form by XMCD.^{20–24} These microscopic variations are very small, and therefore only a small number of results with rather qualitative agreement have been published.^{25–27} Recent XMCD measurements on CrO₂ reveal quantitative consistent results for the MAE using the model by van der Laan.^{15,28} Despite the fact that moment analysis takes care about spectral overlap between the L_2 and L_3 edges,²⁹ the measured spin moment was found to be still reduced. This scalinglike reduction has been identified previously to hybridization and $j_{3/2}$ and $j_{1/2}$ mixing effects.^{15,30,31}

In this paper, we report on the temperature dependence and the corresponding temperature dependent “generation” of the orbital moment and the magnetic dipole term projections of CrO₂. This gives the unique possibility to test the idea of Bruno and the model of van der Laan, without the need of absolute spin-orbit-coupling constants and XMCD spin moment corrections. Therefore, we provide clear and unambiguous evidence for the microscopic origin of the MAE in 3*d* transition metal compounds.

CrO₂ crystallizes in the rutile structure with two equivalent *a* axes (0.4421 nm) and a shorter *c* axis (0.2916 nm).³² The CrO₂ films investigated have been epitaxially grown on isostructural TiO₂ substrates by a chemical vapor deposition technique³³ with a resulting sample thickness of approximately 100 nm. The Curie temperature of the CrO₂ films is 385 K and the films show a (100) orientation. Further details of the sample growth and characterization have been discussed elsewhere.¹²

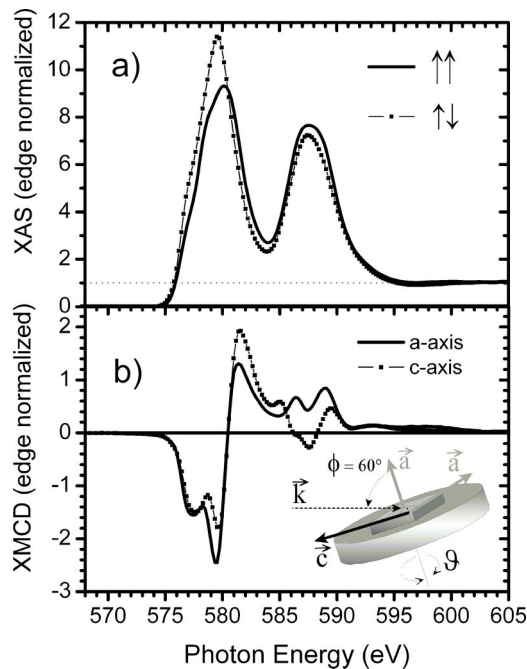


FIG. 1. (a) XAS spectra (edge normalized) for parallel and antiparallel alignment of helicity and external magnetic field at 23 K and c -axis projection. (b) Edge normalized XMCD spectra for enhanced a - and c -axis contributions at 23 K. The inset shows the experimental geometry.

All spectra were recorded in the total electron yield mode at the bending magnet beamline PM I at Bessy II with an energy resolution $E/\Delta E = 2000$ in an applied magnetic field of ± 5 kOe (flipped at each data point). The degree of circular polarization was $95 \pm 3\%$. All spectra are carefully background subtracted and edge normalized using the same background and normalization factor for parallel and antiparallel orientation of the photon beam \vec{k} vector with respect to the sample magnetization. Further details of the experimental setup and data analysis have been published elsewhere.³⁴ X-ray magnetic circular dichroism (XMCD) spectra were taken at a fixed angle of incidence ($\Phi = 60^\circ$) and at two azimuthal angles $\theta = 0^\circ$ and $\theta = 90^\circ$ for enhanced a - and c -axis projections, respectively.

Figure 1(a) shows the normalized XAS spectra for $\theta = 90^\circ$ at 23 K, and Fig. 1(b) the corresponding XMCD spectra for $\theta = 0^\circ$ (a axis) and $\theta = 90^\circ$ (c axis), also at 23 K. The experimental geometry is shown in the inset of Fig. 1(b).

The spectra are nearly identical compared to previous published results.¹⁵ We have measured CrO_2 XMCD in the temperature range from 23 to 330 K at nine temperatures for both crystallographic directions (a and c axis). The spectra are shown in Fig. 2, a axis in (a), c axis in (b) of the figure, with five temperatures omitted for enhanced clarity. Normal sum rule analysis^{20,21} is not suitable to extract magnetic spin moments due to the overlapping features in the XMCD spectra and the absence of a clear separation between the L_2 and L_3 parts. Therefore, we have fitted the spectra by a recently developed moment analysis procedure, which has previously given consistent results for CrO_2 .¹⁵ Moment analysis takes the shape of the spectrum into account and provides the op-

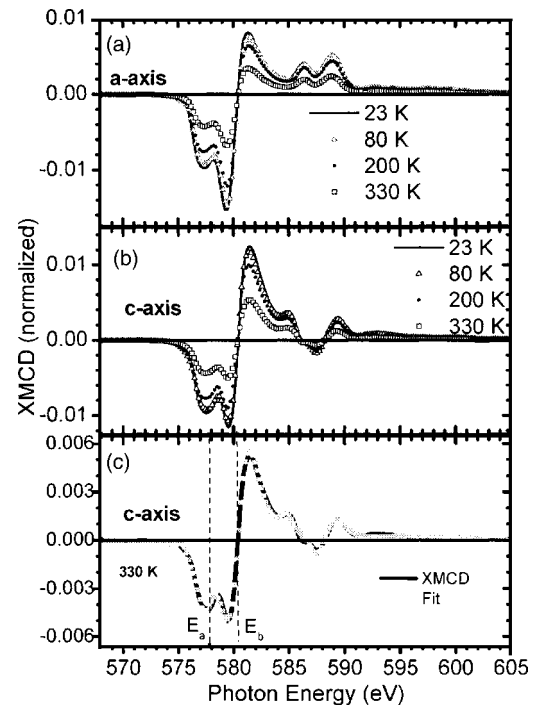


FIG. 2. (a) XMCD spectra for a -axis projection at four different temperatures: 23 (line), 80 (open triangle), 200 (full circle), and 330 K (open square). The spectra are normalized to the resonant absorption signal; (b) XMCD spectra for c -axis projection at four different temperatures: 23 (line), 80 (open triangle), 200 (full circle), and 330 K (open square). The spectra are normalized to the resonant absorption signal; (c) XMCD spectrum for c -axis projection at 330 K (black line) and the corresponding moment analysis fit (grey squares).

portunity to distinguish overlapping features of L_2 and L_3 edges and to separate different parts of the unoccupied band structure. The basic principles, the handling of the fitting routine, and a series of different consistent examples have been recently shown elsewhere.²⁹ In Fig. 2(c) the moment analysis fit at 330 K along the c axis is shown, which reproduces the spectrum nearly perfectly. One important result is the clear separation of the two major parts of the band structure, a small feature near the Fermi energy (E_a at 577.8 eV for the L_3 edge), and a broad feature 3 eV above the Fermi level (E_b at 580.5 eV for L_3 edge). A more detailed discussion of this separation has been given in Refs. 15 and 29. This unusual separation, as well as the antiparallel orbital orientation between the a and b parts, has been demonstrated by recent angular dependent O K edge XMCD results.³⁵

The extracted temperature dependant isotropic total $3d$ spin moment for CrO_2 is shown in Fig. 3(a). The values for the total spin moment are in excellent agreement with former published XMCD results.¹⁵ We have investigated the temperature dependence of the different moments (spin, orbital moment, and T_Z term) and the MAE, and we will prove the validity of the different theoretical models^{18,19} for the generated orbital moment in a nearly quenched system, the T_Z term, and the MAE. We would like to emphasize that also conventional sum rule derived spin and T_Z -term values, without the use of the moment analysis, exhibit the same tem-

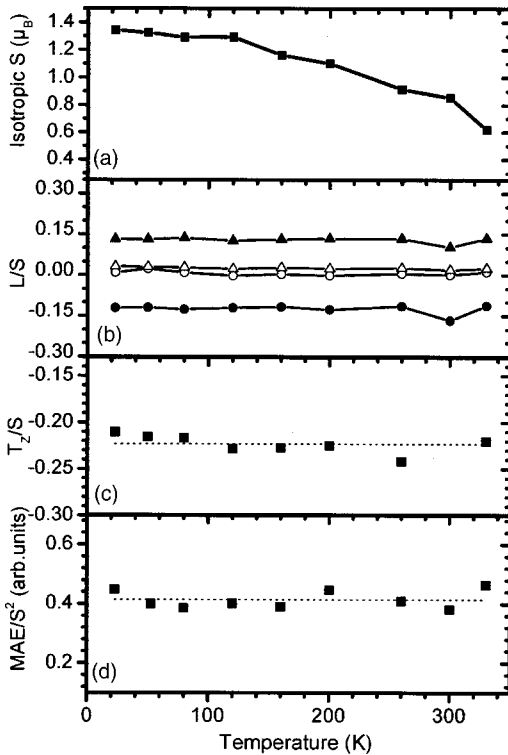


FIG. 3. (a) Temperature dependency of the isotropic total 3d spin moment of CrO_2 per formula unit extracted by XMCD and moment analysis. (b) Temperature dependencies of the ratios of orbital moments per spin moment. The classification of the orbital moments is identical to Ref. 15 (open triangles up: L_a a axis; open circle: L_b a axis; full triangles up: L_a c axis; full circles: L_b c axis). (c) Temperature dependency of the T_Z term per total spin moment. (d) Temperature dependency of the MAE (extracted by XMCD-hysteresis curves) per squared spin moment.

perature dependence with slightly reduced absolute moments.²⁹

As mentioned above, we extracted two contributions to the orbital moment per crystallographic orientation by the moment analysis fitting procedure. The temperature dependencies of the calculated ratios of orbital moment–spin moment are plotted in Fig. 3(b). Following the Bruno model, the orbital moment is described by a tensor equation and generated by the spin moment via an orbital susceptibility: $\bar{L} = Q\bar{S}$ (Refs. 18 and 19). Along the principal axis of this tensor the projection of the orbital moment should be proportional to the spin moment, and the L/S ratio is constant as observed for all four extracted orbital moments. This clearly shows the validity of the model and that the orbital susceptibility is not a function of temperature.

The T_Z term, generated by a quadrupolar spin density distribution, can be separated from the isotropic spin by the use of angular dependent sum rules from Stöhr and König.²⁴ Van der Laan has described the T_Z term as a similar tensor equation of the spin and a quadrupolar charge distribution: $T_Z \approx -2/7Q \cdot \hat{S}$ (Ref. 19), where \hat{S} is a locally acting unit vector along the spin direction and Q is the quadrupole moment of the charge distribution. In a spin only system the expectation value of \hat{S} follows the normalized magnetization

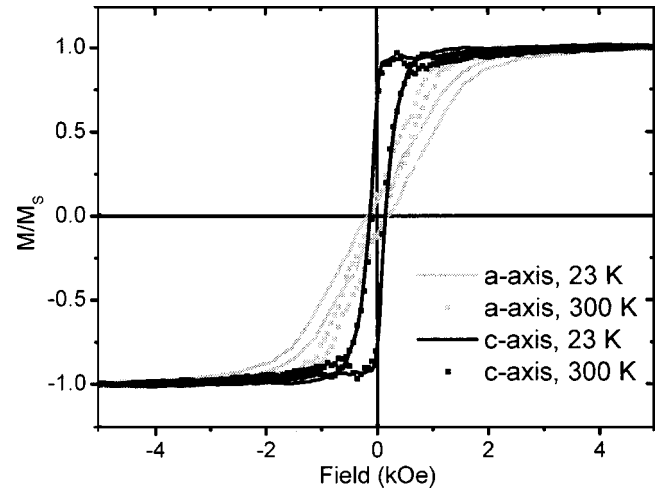


FIG. 4. XMCD-related hysteresis loops at the $\text{Cr } L_3$ edge, selected data shown. The curves for 23 and 300 K are shown for a - and c -axis projections

$\langle \hat{S} \rangle = M(T)/M(0) \propto S(T)$. Along the principal axis the measured ratio T_Z/S should be independent of temperature, similar to the orbital moment. Again, this is clearly observed in our experiment, as shown in Fig. 3(c).

Recently, the important influence of T_Z and L on the MAE has been shown for CrO_2 , and a very good quantitative agreement between the calculated MAE using the van der Laan model and the experimentally extracted MAE (Ref. 15)—derived by *in situ* hysteresis loops (Ref. 36)—has been found.

With the simplified van der Laan formula

$$\delta E \approx -\frac{\xi}{4} \cdot \hat{S} \cdot \{ \langle L^\downarrow \rangle - \langle L^\uparrow \rangle \} + \frac{\xi^2}{\Delta E_{ex}} \frac{21}{2} \cdot \hat{S} \cdot \langle T \rangle,$$

(Ref. 19), omitting the squared diagonal spin-orbit interaction as in Ref. 15, the MAE could be calculated from the microscopic expectation values of L , S , and T_Z . In the formula ξ is the spin-orbit-coupling constant, L^\uparrow is the orbital moment for the majority band (the orbital moment for the empty minority band L^\downarrow vanishes and can be neglected¹⁵), and ΔE_{ex} is the 3d exchange energy. As discussed above $T_Z \propto S$ and $L \propto S$, and, according to the van der Laan formula, the MAE should be $\delta E \propto S^2$. Therefore, we have measured *in situ* XMCD-related hysteresis curves³⁶ and extracted the integral $\int M dH$, and thus the MAE. These are partially shown in Fig. 4, and the ratio of $\text{MAE}/(\text{Spin moment})^2$ is plotted in Fig. 3(d). Due to the fact that the ratio is constant for all data points, we could manifest the applicability of the van der Laan model for the whole temperature regime. The famous $l(l+1)/2$ power law for the MAE, which cannot give a quadratic dependence of the magnetization, worked out by Callen and Callen³⁷ is not in contradiction with our results, because the power law was established for ferromagnetic insulators and in their original work Callen and Callen restrict the law to materials with localized spins and exclude the validity of the law to almost all 3d metals.

In conclusion, we have investigated the halfmetallic ferromagnet CrO₂ using XMCD spectroscopy along two crystallographic axes in a temperature range from 20 to 330 K. We used moment analysis to extract the spin moment, the orbital moment, and the T_Z term and measured *in situ* XMCD-related hysteresis curves to extract the MAE. We have shown that the orbital moments and the T_Z term are proportional to the spin moment and the generation of these two moments is independent of temperature. Van der Laan and Bruno have predicted that the MAE behaves like the spin moment squared.^{18,19} Our experimentally observed pro-

portionality give strong evidence for the microscopic description of the MAE formulated by Bruno, and more recently by van der Laan.

We would like to thank the beam line staff at BESSY II, especially T. Kachel, and A. Schmid for the help during the measurement time. This work was supported by the DFG Forschergruppe Augsburg, Contract No. SCHU 964/4-5 and by the German Federal Ministry of Education and Research (BMBF) Grant No. FKZO5K51PAA/7.

-
- *Author to whom correspondence should be addressed. Eberhard Goering, Max-Planck-Institut für Metallforschung, Heisenbergstrasse 3, 70569 Stuttgart, Germany. FAX: +49 1212-5-116-88-449. Electronic address: goering@mf.mpg.de
- ¹R. A. de Groot, F. M. Mueller, P. G. van Engen, and K. H. J. Buschow, *Phys. Rev. Lett.* **50**, 2024 (1983).
 - ²W. E. Pickett and J. S. Moodera, *Phys. Today* **54**(5), 39 (2001).
 - ³I. I. Mazin, D. J. Singh, and C. Ambrosch-Draxl, *J. Appl. Phys.* **85**, 6220 (1999).
 - ⁴M. A. Korotin, V. I. Anisimov, D. I. Khomskii, and G. A. Sawatzky, *Phys. Rev. Lett.* **80**, 4305 (1998).
 - ⁵S. P. Lewis, P. B. Allen, and T. Sasaki, *Phys. Rev. B* **55**, 10253 (1997).
 - ⁶K. Schwarz, *J. Phys. F: Met. Phys.* **16**, L211 (1986).
 - ⁷Y. Ji, G. J. Strijkers, F. Y. Yang, C. L. Chien, J. M. Byers, A. Anguelouch, G. Xiao, and A. Gupta, *Phys. Rev. Lett.* **86**, 5585 (2001).
 - ⁸R. J. Soulen, J. M. Byers, M. S. Osofsky, B. E. Nadgorny, T. Ambrose, S. F. Cheng, P. R. Broussard, C. T. Tanaka, J. Nowak, J. S. Moodera, A. Barry, and J. M. D. Coey, *Science* **282**, 85 (1998).
 - ⁹Yu. S. Dedkov, M. Fonine, C. König, U. Rüdiger, and G. Güntherodt, *Appl. Phys. Lett.* **80**, 4181 (2002).
 - ¹⁰J. S. Parker, S. M. Watts, P. G. Ivanov, and P. Xiong, *Phys. Rev. Lett.* **88**, 196601 (2002).
 - ¹¹K. Attenkofer and G. Schütz, *J. Phys. IV* **7**, C2 (1997).
 - ¹²M. Rabe, J. Pommer, K. Samm, B. Özyilmaz, C. König, M. Fraune, U. Rüdiger, G. Güntherodt, S. Senz, and D. Hesse, *J. Phys.: Condens. Matter* **14**, 7 (2002).
 - ¹³X. W. Li, A. Gupta, and G. Xiao, *Appl. Phys. Lett.* **75**, 713 (1999).
 - ¹⁴C. B. Stagarescu, X. Su, D. E. Eastman, K. N. Altmann, F. J. Himpsel, and A. Gupta, *Phys. Rev. B* **61**, R9233 (2000).
 - ¹⁵E. Goering, A. Bayer, S. Gold, G. Schütz, M. Rabe, U. Rüdiger, and G. Güntherodt, *Phys. Rev. Lett.* **88**, 207203 (2002).
 - ¹⁶M. Komelj, C. Ederer, and M. Fähnle, *Phys. Rev. B* **69**, 132409 (2004).
 - ¹⁷D. Weller and M. F. Doerner, *Annu. Rev. Mater. Sci.* **30**, 611 (2000).
 - ¹⁸P. Bruno, *Phys. Rev. B* **39**, R865 (1989).
 - ¹⁹G. van der Laan, *J. Phys.: Condens. Matter* **10**, 3239 (1998).
 - ²⁰P. Carra, B. T. Thole, M. Altarelli, and X. Wang, *Phys. Rev. Lett.* **70**, 694 (1993).
 - ²¹B. T. Thole, P. Carra, F. Sette, and G. van der Laan, *Phys. Rev. Lett.* **68**, 1943 (1992).
 - ²²C. T. Chen, Y. U. Idzerda, H. J. Lin, N. V. Smith, G. Meigs, E. Chaban, G. H. Ho, E. Pellegrin, and F. Sette, *Phys. Rev. Lett.* **75**, 152 (1995).
 - ²³G. Schütz, W. Wagner, W. Wilhelm, P. Kienle, R. Zeller, R. Frahm, and G. Materlik, *Phys. Rev. Lett.* **58**, 737 (1987).
 - ²⁴J. Stöhr and H. König, *Phys. Rev. Lett.* **75**, 3748 (1995).
 - ²⁵J. Stöhr, *J. Magn. Magn. Mater.* **200**, 470 (1999).
 - ²⁶D. Weller, J. Stöhr, R. Nakajima, A. Carl, M. G. Samant, C. Chappert, R. Megy, P. Beauvillain, P. Veillet, and G. A. Held, *Phys. Rev. Lett.* **75**, 3752 (1995).
 - ²⁷F. Wilhelm, P. Pouloupoulos, P. Srivastava, H. Wende, M. Farle, K. Baberschke, M. Angelakeris, N. K. Flevaris, W. Grange, J. P. Kappler, G. Ghiringhelli, and N. B. Brookes, *Phys. Rev. B* **61**, 8647 (2000).
 - ²⁸G. van der Laan, *Phys. Rev. B* **55**, 8086 (1997).
 - ²⁹E. Goering, S. Gold, and A. Bayer, *Appl. Phys. A* **78**, 855 (2004).
 - ³⁰J. P. Crocombette, B. T. Thole, and F. Jollet, *J. Phys.: Condens. Matter* **8**, 4095 (1996).
 - ³¹Y. Teramura, A. Tanaka, and T. Jo, *J. Phys. Soc. Jpn.* **65**, 1053 (1996).
 - ³²P. Porta, M. Marezio, J. P. Reimeika, and P. D. Dernier, *Mater. Res. Bull.* **7**, 157 (1972).
 - ³³S. Ishibashi, T. Namikawa, and M. Satou, *Mater. Res. Bull.* **14**, 51 (1979).
 - ³⁴E. Goering, S. Gold, A. Bayer, and G. Schütz, *J. Synchrotron Radiat.* **8**, 434 (2001).
 - ³⁵E. Goering, A. Bayer, S. Gold, G. Schütz, M. Rabe, U. Rüdiger, and G. Güntherodt, *Europhys. Lett.* **58**, 906 (2002).
 - ³⁶E. Goering, A. Fuss, W. Weber, J. Will, and G. Schutz, *J. Appl. Phys.* **88**, 5920 (2000).
 - ³⁷H. B. Callen and E. Callen, *J. Phys. Chem. Solids* **27**, 1271 (1966).